Respiratory Physiology & Neurobiology 175 (2011) 62–69

Contents lists available at ScienceDirect

Respiratory Physiology & Neurobiology

journal homepage: www.elsevier.com/locate/resphysiol

Evaluation and comparison of nasal airway flow patterns among three subjects from Caucasian, Chinese and Indian ethnic groups using computational fluid dynamics simulation

Jian Hua Zhu[a,*], Heow Pueh Lee[a], Kian Meng Lim[a], Shu Jin Lee[b], De Yun Wang[c]

[a] *Department of Mechanical Engineering, National University of Singapore, Singapore*
[b] *Division of Plastic and Reconstructive Surgery, National University Hospital, Singapore*
[c] *Department of Otolaryngology, National University of Singapore, Singapore*

ARTICLE INFO

Article history:
Accepted 14 September 2010

Keywords:
Ethnic group
Nasal cavity
Nasal index
Airflow
CFD

ABSTRACT

Nasal airflow is one of the most important determinants for nasal physiology. During the long evolution of human beings, different races have developed their own attributes of nasal morphologies which result in variations of nasal airflow patterns and nasal functions. This study evaluated and compared the effects of differences of nasal morphology among three healthy male subjects from Caucasian, Chinese and Indian ethnic groups on nasal airflow patterns using computational fluid dynamics simulation. By examining the anterior nasal airway, the nasal indices and the nostril shapes of the three subjects were found to be similar to nasal cavities of respective ethnic groups. Computed tomography images of these three subjects were obtained to reconstruct 3-dimensional models of nasal cavities. To retain the flow characteristics around the nasal vestibules, a 40 mm-radius semi sphere was assembled around the human face for the prescription of zero ambient gauge pressure. The results show that more airflow tends to pass through the middle passage of the nasal airway in the Caucasian model, and through the inferior portion in the Indian model. The Indian model was found with extremely low flow flux flowing through the olfactory region. The sizes of vortexes near the anterior cavity were found to be correlated with the angles between the upper nasal valve wall and the anterior head of the nasal cavity.

1. Introduction

The nasal cavity connects the ambient environment and the pharyngeal portion of the upper airway, providing human beings with warm and humidified air, protecting them from deleterious particles, viruses and bacteria, and enabling them with olfaction. These functions are associated with the airflow in the nasal cavity. The nasal airflow patterns are mainly determined by the nasal morphology and flow rate. Evolutionary adaptation of the nose to climate and natural selection for a suitable nose to facilitate airflow are two important determinants for the variations in shape and dimensions of the nasal airways among different ethnic groups, where "ethnic groups" refers to groups of subjects of different ancestral origins.

The external shapes and dimensions of noses have been studied and compared among different races in various manners. The nasal index, defined as the ratio between nasal breadth and nasal height multiplied by 100, was reported to be different among different races (Davies, 1932; Leong and Eccles, 2009). Using acoustic rhinometry to evaluate the minimum cross-sectional area (MCA), Huang et al. (2001) concluded that there was no significant difference in internal nasal geometry among Chinese, Malays and Indians. Bennett and Zeman (2005) reported that African Americans had a reduced nasal efficiency for uptake of fine particles compared to Caucasians. The nasal airflow rate and pressure drops were observed to be associated with body mass index and gender (Crouse and Laine-Alava, 1999).

Recently, with the advantage of computational fluid dynamics (CFD), the researchers are able to evaluate the detailed flow patterns in human nasal airway by reconstructing models from computed tomography (CT) and Magnetic Resonance Imaging (MRI) scans, which has become a new reliable trend of nasal airflow exploration (Croce et al., 2006; Doorly et al., 2008b; Hörschler et al., 2003; Subramaniam et al., 1998; Wen et al., 2008). Using CFD simulation, mechanisms of airflow, olfactory function, temperature regulation and particle deposition efficiency in human nasal cavity have been studied and evaluated. Segal et al. (2008) reconstructed CFD models of four individuals to study the effects of differences in nasal anatomy on airflow distribution, where significant inter-

---

* Corresponding author at: Dynamics E1-02-01, Department of Mechanical Engineering, National University of Singapore, Faculty of Engineering, 1 Engineering Drive 2, Singapore 117576, Singapore. Tel.: +65 65168934; fax: +65 67791459.
E-mail address: g0800276@nus.edu.sg (J.H. Zhu).

1569-9048/$ – see front matter © 2010 Elsevier B.V. All rights reserved.
doi:10.1016/j.resp.2010.09.008

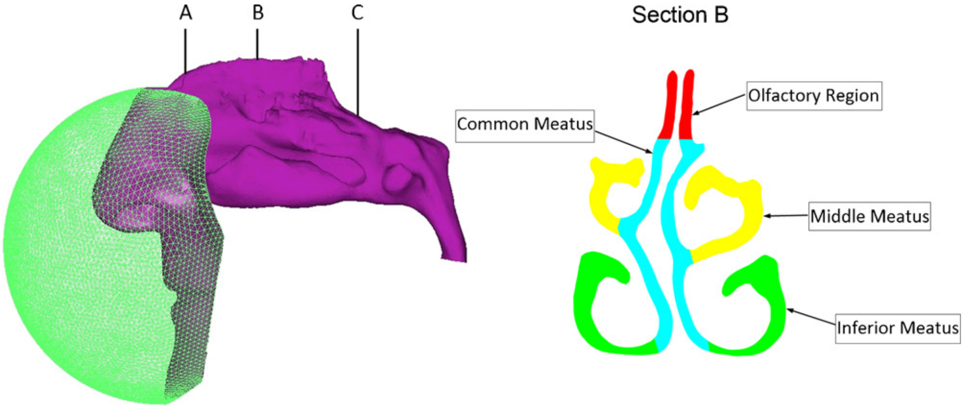

Fig. 1. Model of the nasal cavity (Caucasian). A 40 mm-radius hemi sphere was integrated around the human face. Three cross sections were defined: (A) at the inferior turbinate head; (B) at the middle nasal airway and right below the olfactory bulb; (C) at the end of the turbinates. Four meatuses were defined in section B, namely, the olfactory region, the middle meatus, the inferior meatus and the common meatus.

individual differences in bulk airflow patterns were observed. To our knowledge, few studies have been reported regarding the effects of racial variations of nasal morphology on nasal airflow patterns using CFD simulation.

The present study attempts to evaluate mechanisms of human nasal airflow from different ethnic groups. Three healthy male subjects were selected to obtain CT images and reconstruct 3-dimensional (3D) models of nasal cavities from Caucasian, Chinese and Indian ethnic groups, respectively. CFD simulations were carried out within these models using Fluent (version 6.3.26, 2006 Fluent Inc.). Minute ventilation rate of 7.5 l/min was reported to correspond to human breathing at rest (ICRP, 1994). In this study, inspirational flow rate of 166.7 ml/s (10 l/min) was applied at the nasopharynx to simulate airflow patterns during light breathing. Ensight (version 8.0.7(q), CEI Inc.) was used to evaluate and compare the nasal airway cross sections, flow flux, streamlines and pressure drop among the three cases.

2. Material and methods

2.1. Segmentation of 3D models and mesh generation

The ages of the subjects range between 26 and 41. The interval distances between two consecutive CT images range from 0.5 mm to 0.7 mm for all the three individuals, which are small enough to capture the characteristics of the nasal morphologies during reconstruction of the 3D nasal models.

Mimics (V12.1.0.12 Materialise n.v.) was used to reconstruct the nasal cavity from the original CT scans. A global threshold was firstly applied to segment the nasal cavity from the remaining parts of the images. The resultant segmentation was then manually modified to make the models more representative of the nasal morphology by removing extraneous regions incorrectly identified using a constant threshold level. As Xiong et al. (2008) reported that extremely low airflow passes through the paranasal sinuses during stable respiration (less than 0.05‰ of gross volume flow rate), it would be reasonable to exclude the sinuses from the nasal cavity to simplify the mathematical models in this study. Thereafter, the function of region growing in Mimics was applied to guarantee a consistent lumen. 3D models were then constructed from the segmentation by interpolating. Triangular elements with maximum element length of 1.5 mm were built from the above 3D models which enclosed the whole nasal cavity surface. These elements were further optimized and exported in the file format of Nastran.

Hypermesh (Version 9.0, Altair Engineering Inc.) was used to generate meshes for the models using 3D tetrahedral elements from the above surface triangular elements. As shown in Fig. 1, the nasal cavities were extended by a 40 mm-radius semi sphere which was assembled to totally enclose the nostril entrance. This semi sphere was used to represent natural static air around the human face, which would ensure a realistic inflow condition comparing to applying a zero-pressure boundary condition directly at the nares. Three coronal cross sections were defined along the nasal passage: section A was located near the head of the inferior turbinate; section B was located at the middle nasal airway and right below the olfactory bulb; and section C was located at the end of the middle turbinate. All of these cross sections were created perpendicular to the bottom section. In section B, four meatuses were defined to study the airflow flux distribution, namely the olfactory region, the middle meatus, the inferior meatus and the common meatus. Three prismatic boundary layers were coated around the tetrahedron elements with thickness of 0.1 mm for each layer (approximately 1% of the gross airway width). The triangular element sizes on the semi sphere and the human face around the nostrils were retained 1.5 mm as the shape was relatively smooth and beyond the interesting domain, while the element size on the nasal cavity wall and the nasopharyngeal outlet was refined to 0.6 mm to guarantee the accuracy of the CFD simulation. The triangular elements were optimized according to the skewness, maximum and minimum angles and aspect ratio. Tetrahedron elements and boundary layers were generated and exported in the format of Fluent case file. Fluent was used to solve the laminar Navier–Stokes equations. Ensight was used to analyze the results from Fluent data files.

2.2. Grid independence

Grid independence test was carried out by firstly refining the surface elements of the nasal wall and the outlet using element sizes of 0.8 mm, 0.7 mm, 0.6 mm and 0.55 mm in Chinese model. The element size of hemispherical inlet and the human face was retained 1.5 mm. The total numbers of 3D elements generated according to these surface element sizes are 410,418, 1,345,404, 1,750,428, 2,660,094 and 3,148,381, respectively. As shown in Fig. 2, with zero gauge pressure applying at the hemispheric inlet and 1 m/s velocity magnitude at the outlet, the mean pressure of the outlet and the mean wall shear stress of the whole nasal wall converge as the surface element size approaches 0.6 mm.

Subsequently, the whole surface of the Chinese model (including all the hemispherical inlet, the human face, the nasal wall and the nasopharyngeal outlet) was meshed with element size of 0.6 mm, where 3,975,102 tetrahedron elements were generated.